

# Cavity size influence on Rayleigh-Bénard convection under the effect of wall and gas radiation

Maxime DELORT-LAVAL<sup>1,2\*</sup>, Laurent SOUCASSE<sup>1</sup>, Philippe RIVIERE<sup>1</sup>, Anouar, SOUFIANI<sup>1</sup>

<sup>1</sup>Laboratoire EM2C, CNRS, CentraleSupélec, Université Paris-Saclay  
8-10 rue Joliot Curie, 91192 Gif-sur-Yvette, France

<sup>2</sup>ADEME

155 bis Avenue Pierre Brossolette, Montrouge, 92240, France

\*(Corresponding author: maxime.delort-laval@centralesupelec.fr)

**Abstract** - We investigate Rayleigh-Bénard convection in a cubical cavity filled with humid air under the effect of wall and gas radiation. Coupled direct numerical simulations are carried out for a radiating air/H<sub>2</sub>O/CO<sub>2</sub> mixture at room temperature, using a Chebyshev spectral method for the flow and a ray-tracing method for the radiation field. Three different Rayleigh numbers are studied, from  $Ra = 10^7$  to  $Ra = 10^9$ . Time-averaging is then applied to compare the results, regardless of the multiple flow configurations obtained. Under the Boussinesq approximation, solutions to the uncoupled simulations only depend of the Rayleigh and Prandtl numbers and are not affected by the size of the cavity. However, when radiation is taken into account, coupled results depend on the composition of the gas mixture and the cavity size. In this work we consider a single gas mixture composition and vary the size of the cavity: two cavity sizes are then considered with edges of 1 and 3 meters long. As the cavity size increases, at fixed Rayleigh number, so does the effects of radiation on the flow. The convective flux in the core, as well as the kinetic energy, are increased as radiation is taken into account, and this increase is more important for the larger size of the cavity. The contribution of radiation to the potential energy balance and to the “thermal energy” balance are presented. The large-scale circulation of the fluid settles in vertical mid-planes or diagonal planes depending on the radiation conditions, and reorientations are occasionally observed in the cavity. Radiation affects the large-scale circulation, modifying its structuration and the frequency of reorientations.

## Nomenclature

$a$	thermal diffusivity, $m^2 s^{-1}$	$\Delta T$	temperature difference between the top and bottom walls, K
$g$	gravitational acceleration, $m s^{-2}$	$\nu$	wavenumber, $m^{-1}$
$I$	radiative intensity, $W m^{-2} sr^{-1} cm$	$\nu_f$	kinematic viscosity, $m^2 s^{-1}$
$I^0$	Planck function, $W m^{-2} sr^{-1} cm$	$\kappa$	absorption coefficient, $m^{-1}$
$L$	cavity size, m	$\lambda$	thermal conductivity, $W m^{-1} K^{-1}$
$L$	dimensionless angular momentum	$\theta$	dimensionless temperature
$\mathcal{P}_{rad}$	dimensionless radiative power	$\Omega$	direction
$S$	exchange area, $m^2$	<i>Index and exponent</i>	
$T$	temperature, K	$\nu$	monochromatic
$u$	dimensionless velocity	<i>Dimensionless quantities</i>	
$x$	dimensionless position	Ra	Rayleigh number
<i>Greek symbols</i>		Pr	Prandtl number
$\beta$	thermal expansion coefficient, $K^{-1}$		

## 1. Introduction

It is now well established that radiative transfer has a strong effect on fluid flows in thermally driven natural convection, encountered in various applications such as atmospheric flows, flows in buildings or the cooling of electronical components. The presence of radiation affects the temperature field in the system, which controls the local buoyancy and the motion of the fluid. Since the first numerical studies of the Rayleigh-Bénard flow [1, 2], radiation is known to smooth the temperature field and delay the onset of convection at low Rayleigh numbers. At higher Rayleigh numbers, between  $10^6$  and  $10^9$ , Rayleigh-Bénard flows in confined cubical cavities are characterised by a Large Scale Circulation (LSC) settling either in a drum-like formation, with stream lines in planes parallel to a lateral wall, or in a diagonal plane across the cavity. Intermittent reorientations of the flow are sometimes occurring from one plane to another [3, 4]. However, studies on coupled radiation and convection are scarce in Rayleigh-Bénard configuration, and mostly limited to a gray gas model [5]. Taking into account radiation, and moreover with a real emitting gas model, bears the problem of the dimensionless numbers used to characterize the flow: when radiation is not considered, there are only two parameters (the Rayleigh and Prandtl numbers) controlling the solutions of the Navier-Stokes equations, under the Boussinesq approximation. But when real gas radiation is taken into account, more parameters appear in the equations, among them the optical thickness at different wavenumbers for real molecular gases and, for a given gas mixture and mean temperature, the size of the cavity.

Previous work analysed the influence of radiation in a one-meter-large cubical cavity, filled with a mixture of air and small amount of  $H_2O$  and  $CO_2$  as radiating gas [6, 7]. The present work aims a better understanding of the effects of radiation by enlarging the size of the cavity to a three-meter large cube (more representative of inhabitations), thus increasing the *optical thickness* of the medium.

## 2. Studied configuration and numerical methods

We consider a cubical cavity, heated from the bottom and cooled from the top walls, both being considered isothermal, and black from a radiative perspective. The lateral walls are assumed adiabatic and perfectly reflecting. The cavity is filled with a mixture of air, carbon dioxide ( $X_{CO_2} = 0.001$ ) and water vapour ( $X_{H_2O} = 0.02$ ) at a mean temperature of  $T_0 = 300K$  and at atmospheric pressure ( $\lambda = 6.63 \times 10^{-2} W m^{-1} K^{-1}$ ,  $a = 2.25 \times 10^{-5} m^2 s^{-1}$ ,  $Pr = 0.707$ ). This system is governed by the Navier-Stokes equations under the Boussinesq approximation. In the energy balance, a radiative source term appears, which is obtained by solving the equation of radiative transfer. In the absence of radiative transfer, the solutions of the system only depend on two parameters the Rayleigh (Ra) and Prandtl (Pr) numbers, defined by:

$$Ra = \frac{g\beta\Delta TL^3}{\nu_f a} \quad ; \quad Pr = \frac{\nu_f}{a} \quad (1)$$

The system of equations is solved using a Chebychev spectral method for the Navier-Stokes equations, coupled with a ray-tracing method for radiation. To limit the computational cost of the ray-tracing method, the ADF model is used to describe the radiative properties of the gas [8] and a subgrid model is used to account for the radiation of small spatial scales [9, 10]. Parallelisation of the code is ensured via domain decomposition along the vertical axis for convection, and via the distribution of the rays for radiation.

The reference velocity and time are chosen accordingly to the work of Patterson and Im-

berger [11], and the dimensionless temperature  $\theta$  is defined as follow:

$$u_{ref} = \frac{a\sqrt{Ra}}{L} \quad ; \quad t_{ref} = \frac{L^2}{a\sqrt{Ra}} \quad ; \quad \theta = \frac{T - T_0}{\Delta T} \quad (2)$$

In absence of radiation, these settings allow the dimensionless velocity  $\mathbf{u}$  to remain at the same order of magnitude from  $Ra = 10^6$  and higher. However, when radiation is taken into account, the complex spectrum of the real gas leads to consider a large range of optical thicknesses and the radiative power no longer depends only on dimensionless parameters. For a given molecular composition of the gas, the dimension of the cavity matters.

Three configurations are studied:

- The air is considered dry and radiation is not taken into account. In this case, the size of the cavity doesn't matter and the results only depend on the Rayleigh and Prandtl numbers. This will be referred as the no-radiation case,
- The radiation of the humid air is taken into account, in a cavity with one-meter long edges. This will be referred as the radiation 1m case,
- The radiation of the humid air is taken into account, in a cavity with three-meters long edges. This will be referred as the radiation 3m case.

Direct numerical simulations are carried out for these three cases, for three different Rayleigh numbers:  $Ra = 10^7$ ,  $Ra = 10^8$  and  $Ra = 10^9$ . It is worth noting that, for a given Rayleigh number, increasing the size of the cavity corresponds to a reduction of the temperature difference  $\Delta T$  between the upper and lower walls. After reaching a statistically steady state, numerical integration is carried out for a certain dimensionless time ( $t^+ = t/t_{ref} = 5000$  for  $Ra = 10^7$  and  $Ra = 10^8$ , and  $t^+ = 100$  for  $Ra = 10^9$ ). The results are analysed in terms of statistical average, defined as the combination of averaging over time and over the symmetries of the problem. The complete description of the methodology and numerical details can be found in [7].

### 3. Statistical analysis

Figure 1 shows the temperature, kinetic energy and radiative power (defined as  $\mathcal{P}_{rad} = \mathcal{P}_{absorbed} - \mathcal{P}_{emitted}$ ) vertical profiles at different Rayleigh numbers, for the three cases studied (no-radiation, radiation in 1-meter cavity and radiation in 3-meter cavity), averaged over horizontal planes. In Rayleigh-Bénard convection, the averaged temperature is nearly uniform in the cavity, except in a thin layer of the fluid near the upper and lower walls where a strong temperature gradient is found. Let's consider the lower half of the cavity and, from the lower wall, travel upwards along the vertical axis. When radiation is taken into account, the fluid near the lower wall is strongly emitting, leading to negative radiative power. Because of the convection mixing in the cavity, the temperature gradient is strong near the wall and the fluid is rapidly becoming colder, close to the mean temperature. This colder fluid absorbs a lot of radiation coming from the wall and the fluid near the wall, which corresponds to the hump in radiative power seen in the lower half of the cavity. This heat transfer contributes to increase the thermal gradient in the core of the cavity, in radiative cases, as particularly seen in the radiation 3m case.

This modification of the thermal gradient in the core of the cavity leads to an increase of the potential energy in the radiation case, which contributes to increase the kinetic energy as well. This phenomenon is amplified in the radiation 3m case and will be discussed later (figure 3).

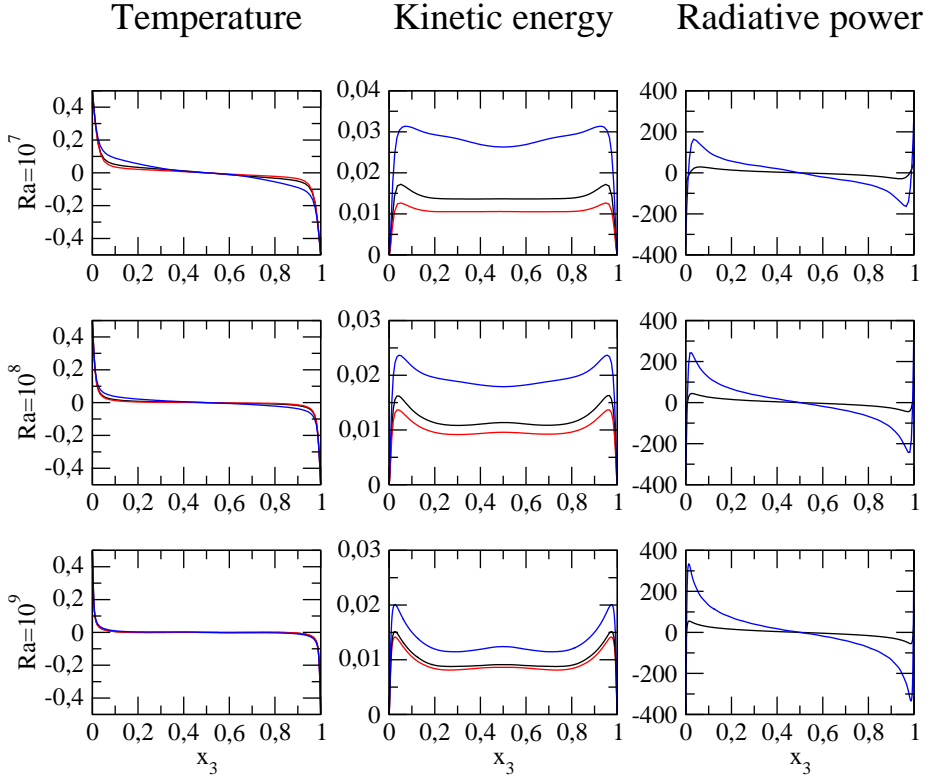


Figure 1 : *Temperature, kinetic energy and radiative power profiles along the vertical axis, averaged over horizontal planes. No radiation (red line), radiation in 1-meter cavity (black line), radiation in a 3-meter cavity (blue line).*

Figure 2 shows the conductive, convective and radiative flux profiles along the vertical axis, averaged over horizontal planes. As the lateral walls are adiabatic, the sum of the different fluxes is constant. In the no-radiation case, there is an equilibrium between conductive and convective fluxes in the cavity. As the temperature gradient is close to zero near the center of the cavity, the conductive flux is close to zero as well, and the convective flux is constant. But the presence of radiation modifies this equilibrium, adding a new term to the balance, which allows a higher convective flux in the center.

Figure 3 displays the kinetic energy ( $e_k = \frac{1}{2}\overline{u_i u_i}$ ), the potential energy ( $e_p = -\text{Pr}\bar{\theta}(x_3 - 0.5)$ ) and the “thermal energy” ( $e_\theta = \frac{1}{2}\bar{\theta}^2$ ), averaged over the whole domain, for the three considered Rayleigh numbers. In all three cases, radiation amplifies the energy level, and the effect is enhanced as the cavity size increases.

As seen in Figures 1, 2 and 3, the effects of radiation increase with the cavity size and decrease with the Rayleigh number. The energy balance writes indeed:

$$\frac{\partial \theta}{\partial t} + u_i \frac{\partial \theta}{\partial x_i} = \frac{1}{\sqrt{\text{Ra}}} \left( \frac{\partial^2 \theta}{\partial x_i \partial x_i} + \mathcal{P}_{\text{rad}} \right), \quad (3)$$

with the dimensionless radiative power defined by

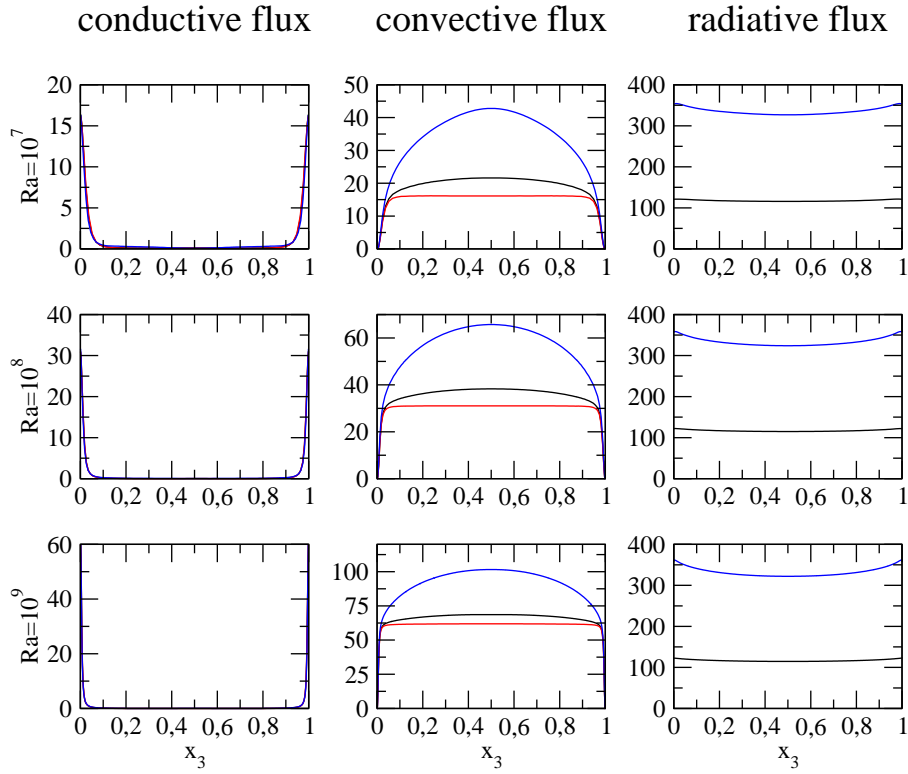


Figure 2 : Conductive, convective and radiative flux profiles along the vertical axis, averaged over horizontal planes. No radiation (red line), radiation in 1-meter cavity (black line), radiation in a 3-meter cavity (blue line).

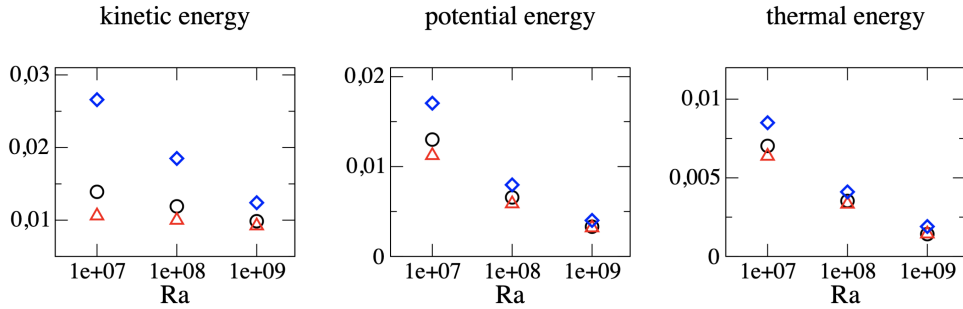


Figure 3 : Total kinetic energy  $\langle e_k \rangle_v$ , potential energy  $\langle e_p \rangle_v$  and “thermal energy”  $\langle e_\theta \rangle_v$  as a function of the Rayleigh number. No radiation (red symbols), radiation in 1-meter cavity (black symbols), radiation in a 3-meter cavity (blue symbols).

$$\frac{1}{\sqrt{Ra}} \mathcal{P}_{\text{rad}}(\mathbf{x}) = \frac{1}{\sqrt{Ra}} \frac{L^2}{\lambda \Delta T} \int_\nu \kappa_\nu \left( \int_{4\pi} I_\nu(\mathbf{x}, \boldsymbol{\Omega}) d\boldsymbol{\Omega} - 4\pi I_\nu^\circ(T(\mathbf{x})) \right) d\nu \quad (4)$$

In the energy budget, the contribution of radiation roughly scales as:

$$\frac{1}{\sqrt{\text{Ra}}} \mathcal{P}_{\text{rad}} = \mathcal{O} \left( \frac{1}{\sqrt{\text{Ra}}} \frac{\kappa_P \sigma T_0^3 L^2}{\lambda} \right) \quad (5)$$

where  $\kappa_P = \int \kappa_\nu I_\nu^0(T_0) d\nu \times \pi / (\sigma T_0^4)$  is the Planck mean absorption coefficient. As the Rayleigh number increases, the relative effect of radiation compared to convection is dampened by the  $\frac{1}{\sqrt{\text{Ra}}}$  factor. However, at a fixed Rayleigh number, the size of the cavity can partly compensate this phenomenon, as the radiative power also scales as  $L^2$ .

Let us consider the kinetic energy: in the no-radiation case, the kinetic energy does not vary significantly. This shows that the reference velocity used to make the velocity dimensionless ( $u_{\text{ref}} = \frac{a\sqrt{\text{Ra}}}{L}$ ), corresponding to a balance between the buoyancy and inertial forces, is well suited for this case. It is not the case, however, when radiation is taken into account, even more when the cavity size increases.

Comparing the 3-meter cavity to the 1-meter cavity, the dimensionless velocity stays at the same order of magnitude: the kinetic energy is less than twice as big at  $\text{Ra} = 10^7$  and about a quarter bigger at  $\text{Ra} = 10^9$ . However, considering the reference velocity  $u_{\text{ref}} = \frac{a\sqrt{\text{Ra}}}{L}$ , which decreases with the cavity size, it means that the corresponding real velocities are smaller in the bigger cavity.

#### 4. Temporal analysis

In cubical Rayleigh-Bénard convection, the Large Scale Circulation (LSC) settles, depending on the Rayleigh number, in a plane parallel to two vertical walls (drum-like flow) or in a diagonal plane of the cube. This can be detected by observing the angular momentum:  $\mathbf{L} = \int (\mathbf{x} - \mathbf{x}_0) \times \mathbf{u} d\mathbf{x}$  of the flow, with respect to the cavity center  $\mathbf{x}_0$ . Figure 4 shows the temporal evolution of the  $x_1$  and  $x_2$  components of the angular momentum. When both  $L_{x_1}$  and  $L_{x_2}$  are non-zero, the flow is in a diagonal plane and, when one of them is zero (in average), it means that the flow is in a drum-like configuration. The usual evolution of the LSC, as the Rayleigh number increases, is from a drum-like circulation (around  $\text{Ra} = 3.10^5$  in the no-radiation case) to a diagonal circulation ( $\text{Ra} \geq 10^6$ ) [6]. At  $\text{Ra} = 10^7$  and  $\text{Ra} = 10^8$ , reorientations of the circulation in another diagonal can be observed, but that have not been observed at  $\text{Ra} = 10^9$ : The flow stabilizes in a diagonal plane. However, this may be due to shorter integration time at higher Rayleigh numbers, caused by the computational cost of the simulation.

When radiation is taken into account, the LSC is delayed in its evolution, compared to the radiation case: at  $\text{Ra} = 10^7$ , in the no-radiation case, the flow is in a diagonal plane, with reorientations. In the 3-meter cavity, the flow is drum-like, as it can be observed at low Rayleigh numbers in no-radiation cases, and in the 1-meter cavity there seems to be an intermediate state between diagonal and drum-like configurations. At  $\text{Ra} = 10^8$ , in the no-radiation case, the flow is also diagonal but with fewer reorientations. In the 3-meter cavity, the flow is mostly drum-like, with short diagonal episodes around  $t^+ = 2000$  and  $t^+ = 2800$ . In the 1-meter cavity, the circulation is diagonal, with some reorientations. At  $\text{Ra} = 10^9$ , the LSC is diagonal and no reorientation are observed in all three cases, maybe due to a too short integration time. Further investigation is required in that area.

The unsteady flow dynamics in the three cases can be further illustrated by snapshots of the

flow fields. Figure 5 displays instantaneous temperature fields close to the bottom wall of the cavity, at  $Ra = 10^9$  and for the three different cases. The presence of radiation does not seem to significantly influence the nondimensional size of the structures of the flow.

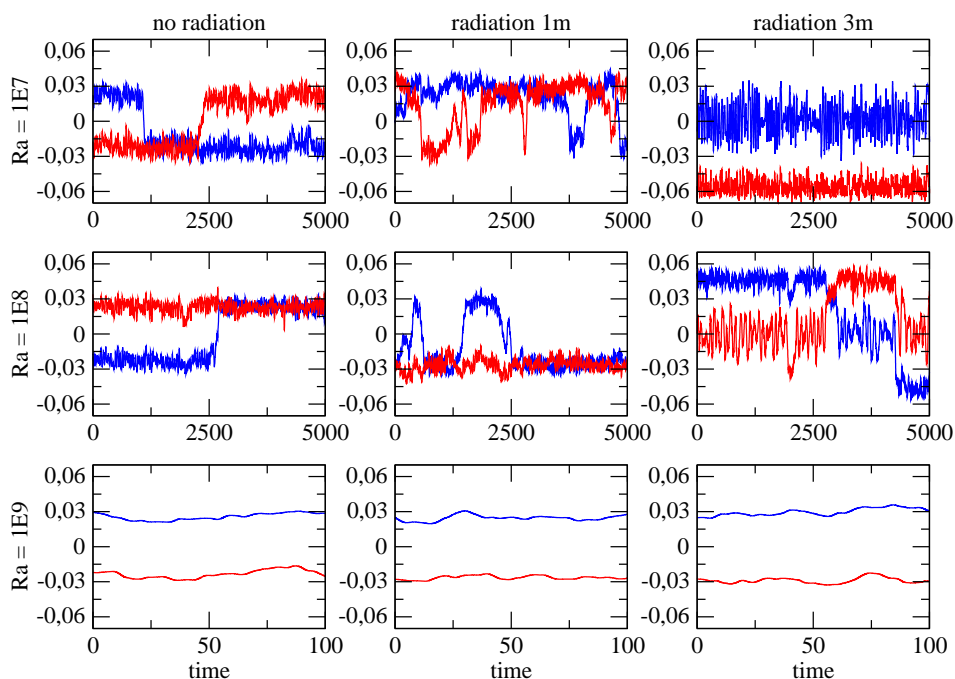


Figure 4 : Time evolution of  $x$  and  $y$  component of the angular momentum  $L_{x_1}$  (blue line) and  $L_{x_2}$  (red line), for different Rayleigh numbers. No radiation (left), radiation in a 1-meter cavity (center), radiation in a 3-meter cavity (right).

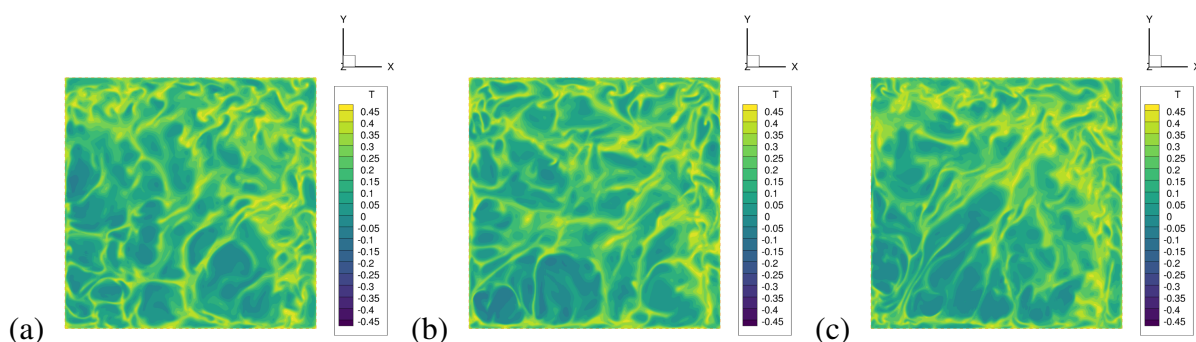


Figure 5 : Snapshots of the temperature field on a plane  $z = 0.007$ , at  $Ra = 10^9$ . No radiation (left), radiation in a 1-meter cavity (center), radiation in a 3-meter cavity (right).

## 5. Conclusion

Taking into account molecular radiative transfer in natural convection requires to introduce several additional parameters, such as optical thickness or the molecular composition of the

fluid, to grasp the complexity of the phenomenon going on. The flow can no longer be characterized only by the Rayleigh and Prandtl numbers, as it is the case in the no-radiation case. When the cavity size increases, the effects of radiation are amplified: the dimensionless radiative source term roughly scales as  $L^2$ . Radiation seems to have two major effects on the flow. At a statistical level, it increases the kinetic energy and the convective flux in the domain. At the LSC level, it seems that it delays the evolution of the circulation regarding the Rayleigh number. Further work will focus on using Proper Orthogonal Decomposition analysis to better understand the effect of radiation, and of the size of the cavity, on the LSC.

## References

- [1] R. M. Goody, The influence of radiative transfer on cellular convection, *Journal of Fluid Mechanics*, 1 (1956) 424-435
- [2] E. A. Spiegel, The smoothing of temperature fluctuations by radiative transfer, *Astrophysical Journal* 126 (1957) 202-207
- [3] N. Foroozani and J. J. Niemela and V. Armenio and K. R. Sreenivasan, Reorientations of the large-scale flow in turbulent convection in a cube, *Physical Review E*, 95 (2017) 033107
- [4] A. Vasiliev and A. Sukhanovskii and P. Frick and A. Budnikov and V. Fomichev and M. Bolshukhin and R. Romanov, High Rayleigh number convection in a cubic cell with adiabatic sidewalls, *International Journal of Heat and Mass Transfer*, 102 (2016) 201-212
- [5] A. Sakurai and R. Kanbayashi and K. Matsubara and S. Maruyama, Radiative Heat Transfer Analysis in a Turbulent Natural Convection Obtained from Direct Numerical Simulation, *Journal of Thermal Science and Technology*, 6 (3) (2011) 449-462
- [6] L. Soucasse and B. Podvin and Ph. Rivière and A. Soufiani, Low-order models for predicting radiative transfer effects on Rayleigh-Bénard convection in a cubic cell at different Rayleigh numbers, *Journal of Fluid Mechanics*, 917 (A5) (2021)
- [7] M. Delort-Laval and L. Soucasse and Ph. Rivière and A. Soufiani, Rayleigh-Bénard convection in a cubic cell under the effects of gas radiation up to  $Ra=10^9$ , *International Journal of Heat and Mass Transfer*, volume (2022 in press) pages
- [8] L. Pierrot and Ph. Rivière and A. Soufiani and J. Taine, A fictitious-gas-based absorption distribution function global model for radiative transfer in hot gases, *Journal of Quantitative Spectroscopy and Radiative Transfer*, 62 (1999) 609-624
- [9] L. Soucasse and Ph. Rivière and A. Soufiani, Subgrid-scale model for radiative transfer in turbulent participating media, *Journal of Computational Physics*, 257, Part A (2014) 442-459
- [10] L. Soucasse and Ph. Rivière and A. Soufiani, Natural convection in a differentially heated cubical cavity under the effects of wall and molecular gas radiation at Rayleigh numbers up to  $3 \times 10^9$ , *International Journal of Heat and Fluid Flow*, 61-B (2016) 510-530
- [11] J. Patterson and J. Imberger, Unsteady natural convection in a rectangular cavity, *Journal of Fluid Mechanics*, 100 part 1 (1980) 65-86

## Acknowledgements

This work benefited from the financial support of the “Agence de l’environnement et de la maîtrise de l’énergie” (ADEME, France). This work was granted access to the HPC resources of IDRIS under the allocation 2020-A0062B00209 attributed by GENCI (Grand Equipement National de Calcul Intensif). This work was also performed using HPC resources from the Mésocentre computing center of CentraleSupélec and École Normale Supérieure Paris-Saclay supported by CNRS and Région Île-de-France (<http://mesocentre.centralesupelec.fr/>).